

LETTER • **OPEN ACCESS**

## Impact of the June 2018 Saddleworth Moor wildfires on air quality in northern England

To cite this article: A M Graham *et al* 2020 *Environ. Res. Commun.* **2** 031001

View the [article online](#) for updates and enhancements.

## Environmental Research Communications



## LETTER

## Impact of the June 2018 Saddleworth Moor wildfires on air quality in northern England

## OPEN ACCESS

## RECEIVED

5 December 2019

## REVISED

28 February 2020

## ACCEPTED FOR PUBLICATION

2 March 2020


## PUBLISHED

13 March 2020

Original content from this work may be used under the terms of the [Creative Commons Attribution 4.0 licence](#).

Any further distribution of this work must maintain attribution to the author(s) and the title of the work, journal citation and DOI.



A M Graham<sup>1,10</sup> , R J Pope<sup>1,2</sup>, J B McQuaid<sup>1</sup> , K P Pringle<sup>1</sup>, S R Arnold<sup>1</sup>, A G Bruno<sup>3,4</sup>, D P Moore<sup>3,4</sup>, J J Harrison<sup>3,4</sup>, M P Chipperfield<sup>1,2</sup>, R Rigby<sup>1,5</sup>, A Sanchez-Marroquin<sup>1</sup> , J Lee<sup>6,7</sup>, S Wilde<sup>6</sup>, R Siddans<sup>8,9</sup>, B J Kerridge<sup>8,9</sup>, L J Ventress<sup>8,9</sup> and B G Latter<sup>8,9</sup>

<sup>1</sup> School of Earth and Environment, University of Leeds, Leeds, United Kingdom

<sup>2</sup> National Centre for Earth Observation, University of Leeds, Leeds, United Kingdom

<sup>3</sup> Department of Physics and Astronomy, University of Leicester, Leicester, United Kingdom

<sup>4</sup> National Centre for Earth Observation, University of Leicester, Leicester, United Kingdom

<sup>5</sup> Centre for Environmental Modelling and Computation, University of Leeds, Leeds, United Kingdom

<sup>6</sup> Department of Chemistry, University of York, York, United Kingdom

<sup>7</sup> National Centre for Atmospheric Science, University of York, York, United Kingdom

<sup>8</sup> Remote Sensing Group, STFC Rutherford Appleton Laboratory, Chilton, United Kingdom

<sup>9</sup> National Centre for Earth Observation, STFC Rutherford Appleton Laboratory, Chilton, United Kingdom

<sup>10</sup> Author to whom any correspondence should be addressed.

E-mail: [ee15amg@leeds.ac.uk](mailto:ee15amg@leeds.ac.uk)

**Keywords:** wildfire, earth observation, air quality, aircraft observations, TROPOMI, FAAM, AURN

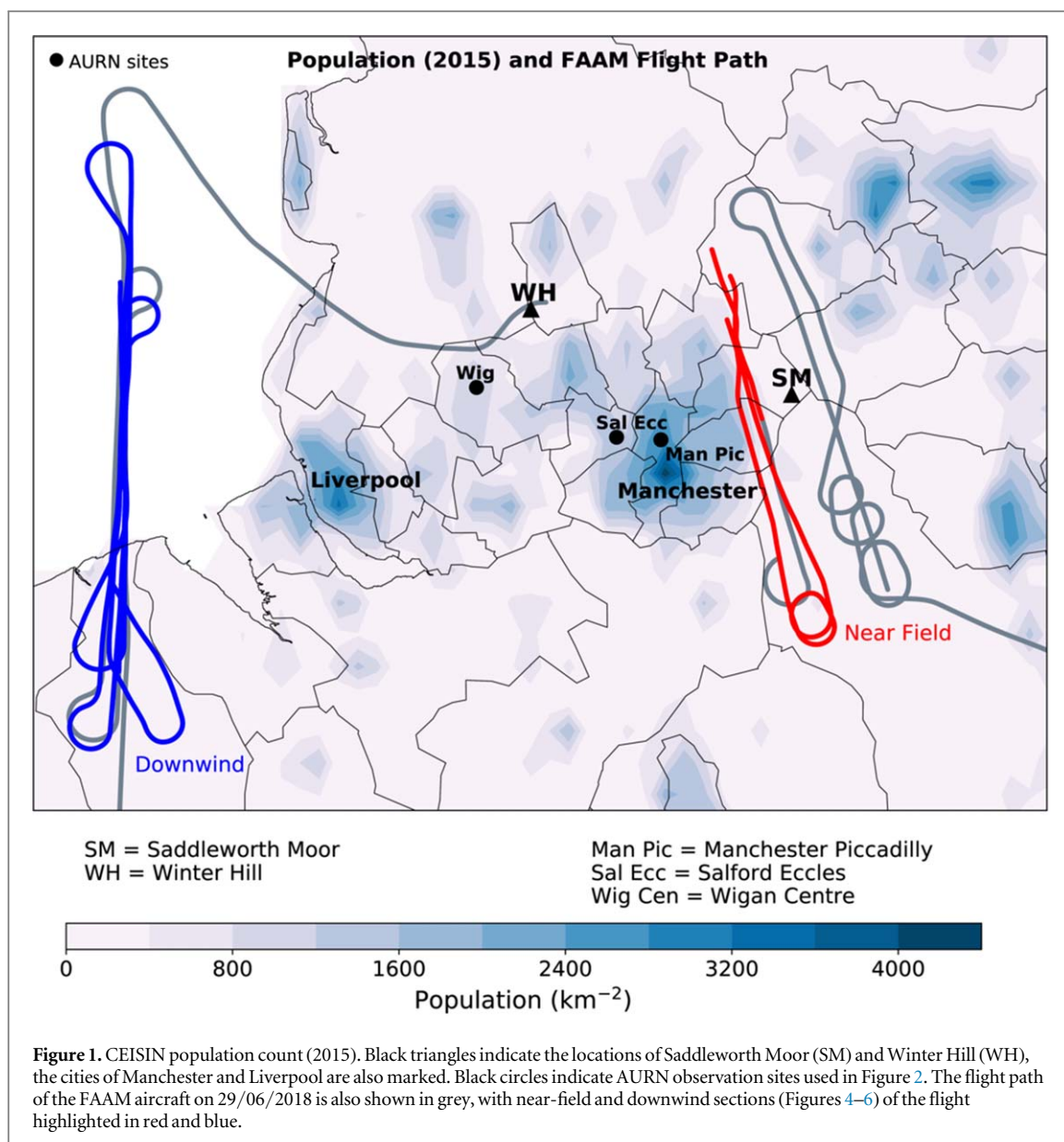
Supplementary material for this article is available [online](#)

## Abstract

The June 2018 Saddleworth Moor fires were some of the largest UK wildfires on record and lasted for approximately three weeks. They emitted large quantities of smoke, trace gases and aerosols which were transported downwind over the highly populated regions of Manchester and Liverpool. Surface observations of PM<sub>2.5</sub> indicate that concentrations were 4–5.5 times higher than the recent seasonal average. State-of-the-art satellite measurements of total column carbon monoxide (TCCO) from the TROPOMI instrument on the Sentinel 5—Precursor (S5P) platform, coupled with measurements from a flight of the UK BAe-146–301 research aircraft, are used to quantify the substantial enhancement in emitted trace gases. The aircraft measured plume enhancements with near-fire CO and PM<sub>2.5</sub> concentrations >1500 ppbv and >125 μg m<sup>-3</sup> (compared to ~100 ppbv and ~5 μg m<sup>-3</sup> background concentrations). Downwind fire-plume ozone (O<sub>3</sub>) values were larger than the near-fire location, indicating O<sub>3</sub> production with distance from source. The near-fire O<sub>3</sub>:CO ratio was (ΔO<sub>3</sub>/ΔCO) 0.001 ppbv/ppbv, increasing downwind to 0.060–0.105 ppbv/ppbv, suggestive of O<sub>3</sub> production enhancement downwind of the fires. Emission rates of CO and CO<sub>2</sub> ranged between 1.07 (0.07–4.69) kg s<sup>-1</sup> and 13.7 (1.73–50.1) kg s<sup>-1</sup>, respectively, similar to values expected from a medium sized power station.

## 1. Introduction

Vegetation fires contribute a large source of trace gases and aerosols into the Earth's atmosphere (Lobert and Warnatz 1993, Helas and Pienaar 1996, Cheng *et al* 1998, Reddington *et al* 2014, Peterson *et al* 2018, Wooster *et al* 2018), which have substantial implications for climate (Liu *et al* 2014, Núñez *et al* 2014, Sommers *et al* 2014, Hamilton *et al* 2018, Rowlinson *et al* 2019) and air quality (AQ) (Konovalov *et al* 2011, Reddington *et al* 2015, Moore (2019), Bravo *et al* 2002, Phuleria *et al* 2005). Unlike many fire-prone regions, vegetation fires in the United Kingdom (UK) are relatively small and rare (Van Der Werf *et al* 2017, Davies *et al* 2016, Yallop *et al* 2006). However, on the June 24th 2018, large-scale wildfires broke out for approximately three weeks over Saddleworth Moor and Winter Hill, in north west England (BBC, 2018), requiring over 100 firefighters to tackle the blaze



(Day and Green, 2018). At their peak, the Saddleworth Moor fires covered approximately  $8 \text{ km}^2$  of moorland (Information Officer, Greater Manchester Combined Authority GMCA (2019)), representing the largest wildfires close to an urban population in the UK on record (Figure 1) (Center for International Earth Science Information Network—CIESIN—Columbia University (2018)). Therefore, this provided the first opportunity to measure the mixing of fire emissions with anthropogenic emissions in the UK. The fires forced the evacuation of several dozen properties and closure of many schools (Pidd and Rawlinson, 2018). The fires primarily burned heather-dominated moorland with an underlying area of dry peat (Bain *et al* 2011, Xu *et al* 2018, Information Officer, Greater Manchester Combined Authority GMCA (2019)). Flames ranged between to 2–4 m in height, depending on the overlying vegetation type and wind conditions (Information Officer, Greater Manchester Combined Authority GMCA (2019)). Fires also propagated vertically and laterally through the peat layer, which would be expected to lead to large emissions of greenhouse gases and air pollutants (Wooster *et al* 2018). As peat is a substantially oxygenated fuel source, it can burn underground for long periods (e.g. weeks to months (Hu *et al* 2018, Roulston *et al* 2018)) making peat fires extremely difficult to control. Emissions from peat are poorly understood but it is thought that during the flaming stage, fires emit large amounts of soot and nitrogen oxides ( $\text{NO}_x$ ), while in the smouldering stage they emit much more carbon monoxide (CO), methane ( $\text{CH}_4$ ), volatile organic compounds (VOCs) and particulate matter (PM) (Turetsky *et al* 2015).

Throughout the period of June 22nd to 29th, meteorological conditions were favourable for the development and spread of the Saddleworth Moor and Winter Hill fires. Between June 22nd and 29th 2018, the UK experienced strong anticyclonic conditions from enhancement of the Azores high pressure system in the North Atlantic. Mean sea level pressure (MSLP) and geopotential height at 850 hPa (850GPH), from ERA-

Interim and ERA5 reanalysis, indicate the stable high-pressure system (MLSP > 1020 hPa and 850GPH 1560–1600 m over northern England) resulted in low 10 m wind speeds ( $<5 \text{ m s}^{-1}$ ) and high surface temperatures ( $\sim 27^\circ\text{C}$  on June 26th) (ERA-Interim, ECMWF), which dried out vegetation and reduced the likelihood of precipitation (see supplementary material, SM1 and figures S1–3 is available online at [stacks.iop.org/ERC/2/031001/mmedia](https://stacks.iop.org/ERC/2/031001/mmedia)). In the future, conditions such as this are likely to become more common within the UK (Guerreiro *et al* 2018). Projections suggest that, as a result, UK wildfires are likely to become more frequent and intense (Albertson *et al* 2010) yielding more hazardous AQ situations in nearby populated areas.

Visible images between the June 25th to 30th, from the Moderate Resolution Imaging Spectroradiometer (MODIS) instruments, on-board NASA's Aura and Terra satellites, clearly show fire initiation followed by a westward propagation of the fire smoke plume (see figure S4). Following the substantial visible impact (i.e. smoke and burned area) of the Saddleworth Moor and Winter Hill fires and the related high-level media coverage, we use state-of-the-art satellite observations from the newly launched (October 2017) TROPOMI instrument on-board ESA's Sentinel-5 Precursor (S5P), which provides, for the first time, high resolution observations of trace gases to quantify the impact of the pollutants from fires from space. We combine these observations with ground and specialised aircraft campaign observations to investigate the influence these fires had on atmospheric composition and AQ across north-western England. Section 2 describes the observations used, section 3 presents our results and section 4 summarises the implications of our findings.

## 2. Data and methods

### 2.1. Automated urban and rural network observations

Surface observations of particulate matter ( $\text{PM}_{2.5}$ —atmospheric aerosol with a diameter less than 2.5 microns) are taken from Manchester Piccadilly, Salford Eccles and Wigan Centre Automated Urban and Rural Network (AURN) sites (DEFRA, 2019). AURN is the largest automated air quality monitoring network in the UK with 145 sites. These sites use the FDMS (Filter Dynamics Measurement System) analyser, which is based on the TEOM (Tapered Element Oscillating Microbalance), (Department for Environment, Food and Rural Affairs DEFRA (2008)). Air is drawn in through inlets for  $\text{PM}_{2.5}$  and  $\text{PM}_{10}$  where it is dried and weighed on a filter held at  $30^\circ\text{C}$ . This system measures non-volatile and volatile fractions by cycling through cold and warm chambers to evaporate volatile species before re-weighing the sample. Further information on data quality checks and uncertainties can be found in AEAT (2009). We use daily mean  $\text{PM}_{2.5}$  concentrations (calculated from hourly measurements, where > 75% of hourly measurements each day are available) for June 16th to July 12th 2013–2018 to assess the impact of the fires on downwind populated areas (e.g. Manchester Piccadilly, Salford Eccles and Wigan) (see figure 1) and to compare with longer term averages for the particular time of year.

### 2.2. Satellite observations

Satellite measurements of total column carbon monoxide (TCCO) and tropospheric column nitrogen dioxide ( $\text{TCNO}_2$ ) are obtained from the TROPOMI instrument on-board ESA's Sentinel-5 Precursor (S5P) satellite (Veefkind *et al* 2012). S5P was launched in October 2017 into a sun-synchronous polar orbit with a local overpass time of 13:30 (Veefkind *et al* 2012). The instrument has a nadir-viewing spectral range of 270–500 nm (ultraviolet-visible, UV-vis), 675–775 nm (near-infrared, NIR) and 2305–2385 nm (short wave-infrared, SWIR). TROPOMI represents the next generation of satellite instruments for observing global and regional AQ (Pope *et al* 2019) with an unparalleled nadir horizontal spatial resolution of  $3.5 \text{ km} \times 7.0 \text{ km}$  for UV-NIR bands and  $7.0 \text{ km} \times 7.0 \text{ km}$  for SWIR bands. For comparison, its predecessor, the Ozone Monitoring Instrument (OMI), had a horizontal spatial resolution of  $24 \text{ km} \times 13 \text{ km}$  (Boersma *et al* 2011). We also use fire radiative power (FRP) data from the MODIS instruments on-board NASA's Aqua and Terra satellites, launched in 1999 and 2002, respectively. Both instruments are nadir viewing (spectral range,  $0.41\text{--}15 \mu\text{m}$ ) with sun-synchronous local overpass times of 10:30 and 13:30, respectively (Remer *et al* 2005). The approach of Pope *et al* (2018) is used to map TROPOMI TCCO data onto a  $0.03^\circ \times 0.03^\circ$  grid over the UK, while the FRP data (Level 3 product) is on a  $0.1^\circ \times 0.1^\circ$  grid.

Garane *et al* (2019) find a typical global bias of 0%–1.5% between TROPOMI TCCO and surface validation sites. For the Saddleworth Moor fires, we see precision errors of approximately 3.3%–4.3%. Further information on the instrumentation and uncertainties can be found in Lambert *et al* (2019).

### 2.3. FAAM aircraft data

The UK's BAe-146–301 Large Atmospheric Research Aircraft flew on June 29th 2018 to target the Saddleworth Moor fires (flight number C110). The aircraft is operated by the Facility for Airborne Atmospheric Measurements (FAAM, Ryder *et al* 2015) and detailed information on the aircraft instrumentation and their uncertainties is given by Harris *et al* (2017). For this flight, *in situ* measurements of carbon monoxide (CO),

ozone (O<sub>3</sub>) nitrogen dioxide (NO<sub>2</sub>) and particulate matter with a diameter less than 2.5 μm (PM<sub>2.5</sub>) amongst other species, were obtained.

PM<sub>2.5</sub> data is calculated from data collected by optical particle counters mounted under the wing that measure aerosol size distributions. The instruments used were the passive cavity aerosol spectrometer probe 100-X (PCASP). The PCASP measures particles in the 0.1–3 μm diameter size range. Further information on the method the instruments used to calculate aerosol diameter and the calibration method used is described in Rosenberg *et al* (2012). We find uncertainty within the integrated volume in the PM<sub>2.5</sub> range dataset to be ~30%–35% at the 1-sigma confidence interval. Further information on sources of these uncertainties can be found in the Supplementary Material SM 7.

Measurements of NO were made using a custom built chemiluminescence instrument (Air Quality Design Inc.), with NO<sub>2</sub> measured on a second channel by photolytic conversion to NO at 395 nm using a blue light converter (BLC), followed by detection by chemiluminescence (Lee *et al* 2009). Estimated accuracies are 4% for NO 5% for NO<sub>2</sub>, with associated precision of 31 and 45 pptv respectively (for 1 Hz data). Further information is in the supplementary material SM 7.

Ozone was measured by an ultraviolet (UV) absorption photometer (Thermo Fisher, model 49 C) with an uncertainty of 2% and a precision of 1 ppb for 4-s measurements (Harris *et al* 2017). CO was measured by a vacuum UV fluorescence analyzer (Aero Laser GmbH, model AL5002; Gerbig *et al* (1999)). The instrument was calibrated in flight every ~45 min using a synthetic-air working standard (Air Liquide, ~500 ppb). The 1-Hz CO measurements have a 2% uncertainty and 3-ppb precision (Harris *et al* 2017)

The aircraft left Cranfield, Bedfordshire at approximately 10:00 UTC, then undertook targeted fire plume measurements over Saddleworth Moor (near-field) at 10:30–11:30 UTC (figures S9 and 4(a)) before taking downwind measurements over the Irish Sea (12:00–13:00 UTC). The aircraft returned to Cranfield around 15:00 UTC.

### 3. Results

#### 3.1. MODIS visible images

MODIS visible images (Figure S4) clearly show the ignition and time-evolution of the Saddleworth Moor and Winter Hill fires. Fire ignition occurs on June 25th 2018 on Saddleworth Moor. The smoke plume initially moves northwards (26th June) before shifting westwards, propagating over Manchester and Liverpool (27th–30th June). The size of the smoke plume peaks on 27th June. The Winter Hill fire then begins on June 30th and propagates westwards towards the Lancashire coast.

#### 3.2. Automated urban and rural network observations

Observations of surface PM<sub>2.5</sub> at the Manchester Piccadilly, Salford Eccles and Wigan Centre AURN sites show enhanced concentrations during the fire period (grey shading in Figure 2). At all sites, daily mean PM<sub>2.5</sub> concentrations peak above 40 μg m<sup>-3</sup> (black dashed line), which is substantially larger than concentrations before and after the fire event (note Manchester Piccadilly is the only site where July 2018 data was available). These concentrations are well above the World Health Organisation (WHO) 24-h guideline limit of 25 μg m<sup>-3</sup>, highlighting the potential population exposure risks even over this short time period.

We also use volatile and non-volatile PM<sub>2.5</sub> observations to investigate the relative influence of the primary and secondary components of PM<sub>2.5</sub> from the fire. Non-volatile PM<sub>2.5</sub> comprises of unreactive solid particles (e.g. elemental carbon, primary organic aerosol) (Chowdhury *et al* 2007, Tian *et al* 2009) whereas volatile PM<sub>2.5</sub> comprises of gaseous reactive precursors (e.g. sulfate, nitrate and VOCs) which can switch between the gas and solid phase through condensation. Considerable uncertainties exist in the apportionment of fire-emitted PM<sub>2.5</sub> due to the complex range of factors controlling emissions, which include fuel type, fuel moisture content and organic aerosol mass concentration. Here, the AURN measurements indicate that during the Saddleworth Moor fires non-volatile PM<sub>2.5</sub> was strongly correlated with total PM<sub>2.5</sub> during the fire period. In 2018, the non-volatile fraction of total PM<sub>2.5</sub> is between 3 and 18% higher than between 2013 and 2017, contributing to up to 93% of total PM<sub>2.5</sub> (see table S1). Compared with previous years (June 2013–2017 observational spread), the non-volatile PM<sub>2.5</sub> concentrations are 4–5.5 times higher than average.

#### 3.3. TROPOMI observations

The time evolution (25th–30th June) of the Saddleworth Moor and Winter Hill fires can also clearly be seen in the TROPOMI TCCO data where the fire plume propagates westwards (top six panels of figure 3) over Manchester and Liverpool (blue circles). Over Saddleworth Moor, TCCO peaks at over 0.04–0.05 moles m<sup>-2</sup> (26th and 27th June) with background concentrations of 0.02–0.025 moles m<sup>-2</sup>. Between June 27th–29th the plume has dispersed westwards with ‘in-plume’ concentrations remaining above 0.030 moles m<sup>-2</sup>. By the 30th

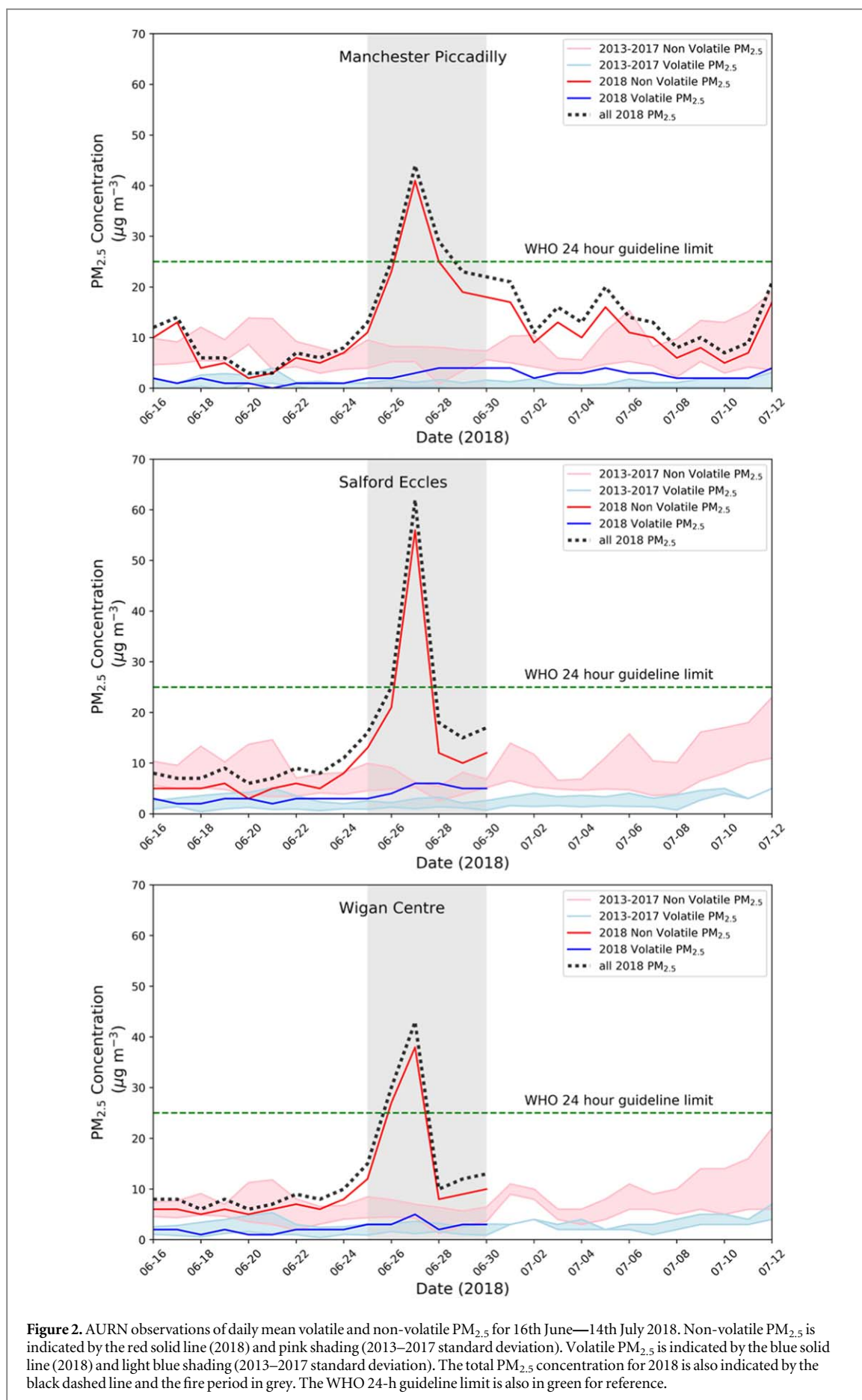
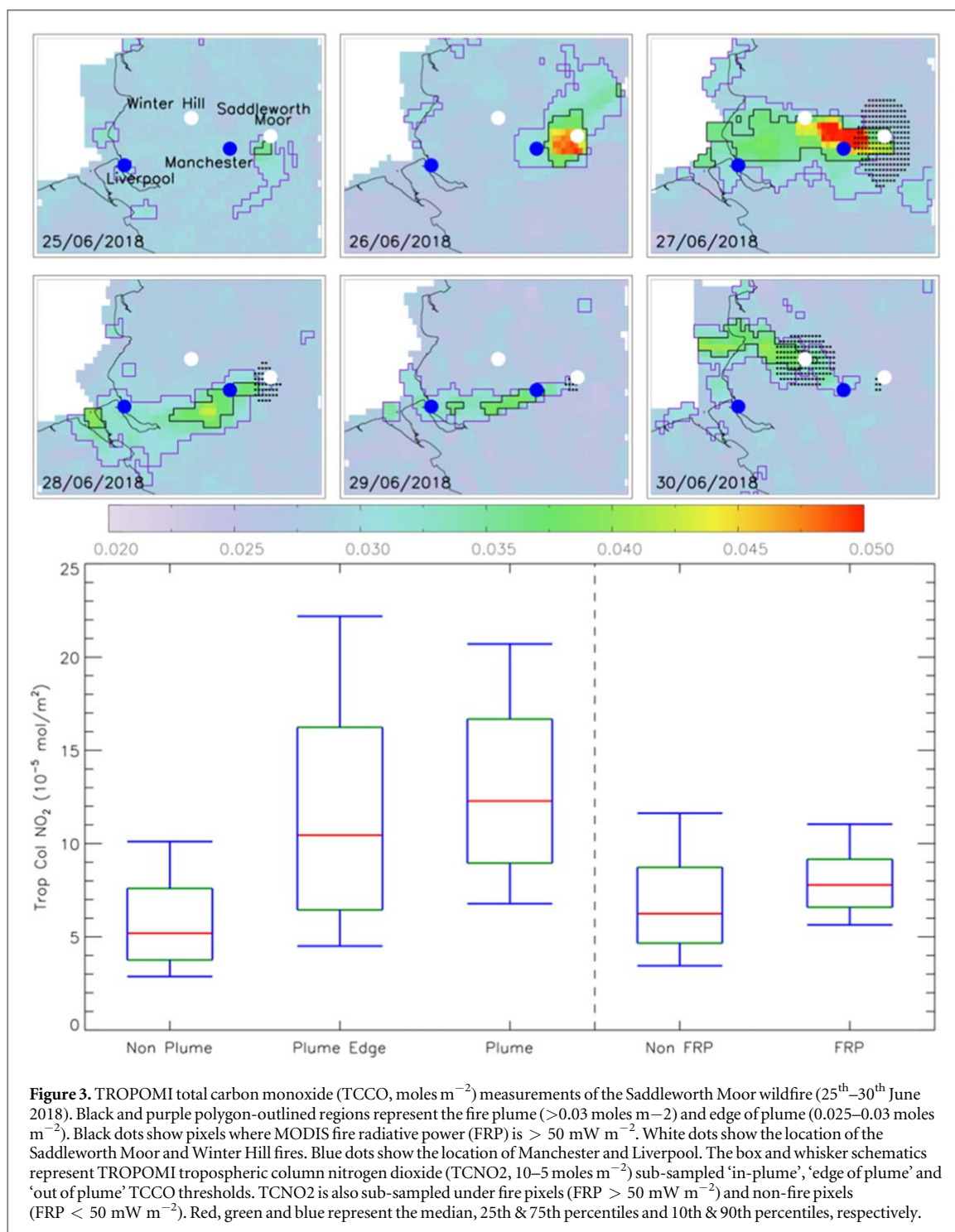


**Figure 2.** AURN observations of daily mean volatile and non-volatile  $PM_{2.5}$  for 16th June—14th July 2018. Non-volatile  $PM_{2.5}$  is indicated by the red solid line (2018) and pink shading (2013–2017 standard deviation). Volatile  $PM_{2.5}$  is indicated by the blue solid line (2018) and light blue shading (2013–2017 standard deviation). The total  $PM_{2.5}$  concentration for 2018 is also indicated by the black dashed line and the fire period in grey. The WHO 24-h guideline limit is also in green for reference.



June, the Saddleworth Moor plume has diminished but the Winter Hill fires have fully developed with a north-westerly plume direction (TCCO  $> 0.04$  moles  $m^{-2}$ ). The time-evolution of the TCCO plume correlates strongly with the MODIS visible images (see Figure S4) supporting the robustness of the novel TROPOMI composition data. This is also seen in TCCO data from the Infrared Atmospheric Sounding Interferometer (IASI) satellite (see SM 8 and Figure S14), further supporting TROPOMI. As TCCO enhancements flow out over Manchester and Liverpool, both densely populated, there will likely be substantial increases in other prominent air pollutants (e.g. NO<sub>2</sub>, PM<sub>2.5</sub> and O<sub>3</sub>) as shown in Figure 2.

Inspection of the TROPOMI TCNO<sub>2</sub> data (see SM5 and Figure S7) highlights concentration enhancements over both Manchester and Liverpool during the Saddleworth Moor fire time period. However, the prevailing anticyclonic meteorological conditions have been shown in other studies (e.g. Pope *et al* 2014 and 2015) to significantly increase NO<sub>2</sub> concentrations over urban regions due to accumulation of anthropogenic emissions. Therefore, to isolate potential fire-sourced NO<sub>2</sub> signal, a quantitative classification of ‘fire-influenced’ pixels was

used to sub-sample the TCNO<sub>2</sub> data. Firstly, satellite pixels with FRP > 50 mW m<sup>-2</sup> were classed as ‘fire’ (black circles in Figure 3), while those with FRP < 50 mW m<sup>-2</sup> were classed as ‘non-fire’. Secondly, the TCCO was used to identify the observations as ‘in-plume’ (TCCO > 0.03 moles m<sup>-2</sup>, black polygon-outlining—figure 3), ‘edge of plume’ (0.025 moles m<sup>-2</sup> < TCCO < 0.030 moles m<sup>-2</sup>, purple polygon-outlining) and ‘out of plume’ (0.020 moles m<sup>-2</sup> < TCCO < 0.025 moles m<sup>-2</sup>). The ‘out of plume’ lower limit was set to 0.020 moles m<sup>-2</sup> to ensure that near-plume satellite pixels are used and not background pixels across the domain. Several different thresholds were tested and this combination yielded the most realistic spatial plume distributions when compared to MODIS visible images.

When sub-sampled under ‘fire’ pixels (bottom panel, Figure 3) the median TCNO<sub>2</sub> concentration is approximately  $8.0 \times 10^{-5}$  moles m<sup>-2</sup>, which is significantly larger than the ‘non-fire’ pixel TCNO<sub>2</sub> median ( $6.0\text{--}7.0 \times 10^{-5}$  moles m<sup>-2</sup>) (95% confidence level (CL) based on student t-test, using the mean). The ‘fire’ TCNO<sub>2</sub> 10th, 25th and 75th percentile concentrations are also larger than the non-fire-TCNO<sub>2</sub> equivalent. However, the ‘non-fire’ TCNO<sub>2</sub> 90th percentile value is marginally larger. The TCNO<sub>2</sub> data sub-sampled under the TCCO plume definitions show a similar pattern. ‘Out of plume’ median TCNO<sub>2</sub> is the lowest ( $5\text{--}6 \times 10^{-5}$  moles m<sup>-2</sup>) of all classifications (also true for the 10th, 25th, 75th and 90th percentiles). Though downwind of the fire location, the ‘edge of plume’ and ‘in plume’ classifications have the largest median TCNO<sub>2</sub> values of  $10.0\text{--}11.0 \times 10^{-5}$  moles m<sup>-2</sup> and  $12.0\text{--}13.0 \times 10^{-5}$  moles m<sup>-2</sup>, respectively. These two classifications both overlap regions of enhanced anthropogenic NO<sub>2</sub> sources (i.e. Manchester and Liverpool), so their median and percentile concentrations are larger (see SM5 and Figure S7). By using the TCCO data as a tracer for the fire plume, we detect a NO<sub>2</sub> fire response on top of the anthropogenic NO<sub>2</sub> signal. This is supported by aircraft results in section 3.5.1, though we note that there is a substantial level of noise in the TROPOMI NO<sub>2</sub> data (unlike for CO). Here, the median and percentile concentrations are all larger ‘in plume’ than ‘edge of plume’ where the medians are significantly different at the 95% CL (student t-test, using the mean). This indicates that the increased spatial resolution of TROPOMI (when compared to previous satellites such as OMI) is able to both, detect the impacts of fires on air pollutants and to quantify them, something not possible with the sparse coverage of the AURN sites. We can therefore conclude that the Saddleworth Moor and Winter Hill fires, observed by TROPOMI, significantly enhanced observed NO<sub>2</sub> and CO concentrations.

### 3.4. FAAM aircraft observations

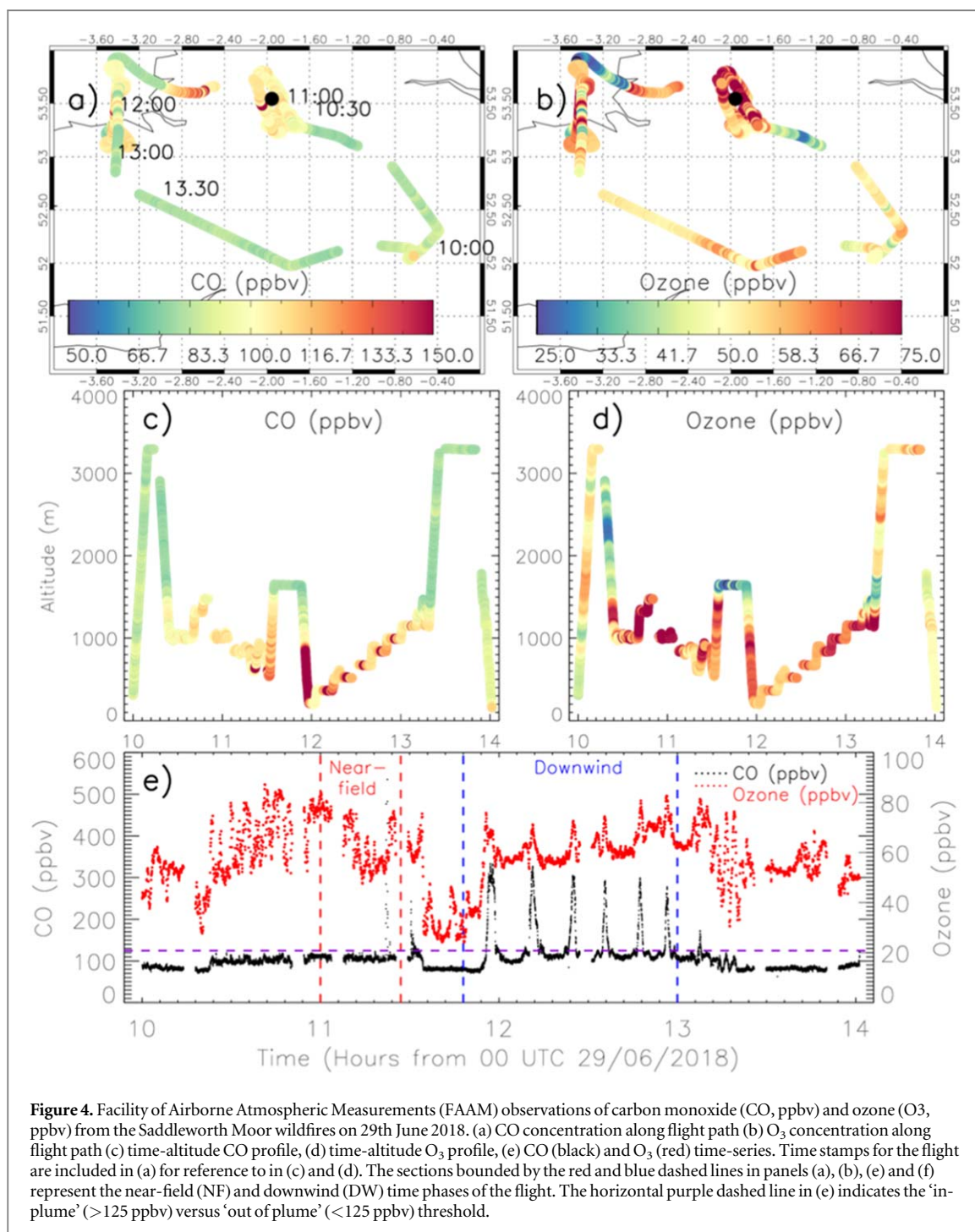
#### 3.4.1. Pollutant concentrations ‘in-plume’ and ‘out-of-plume’ near-field and downwind

To verify the satellite results and investigate other air pollutants, we use FAAM aircraft observations of CO, PM<sub>2.5</sub>, O<sub>3</sub> and NO<sub>2</sub>, from June 29th 2018. Between approximately 11:00–11:30 UTC the aircraft was sampling the near-field fire plume southwest-west of Saddleworth Moor (black circle—Figures 4(a) and (b)) at 500–1000 m above ground level (AGL). Measurements within the plume show enhanced CO concentrations peaking at over 1500 ppbv, while background CO ranged between 80–100 ppbv (Figures 4(c) and (e)). This correlates well with measurements of PM<sub>2.5</sub> aerosol concentration, which also indicate enhanced PM<sub>2.5</sub> in the plume ( $15\text{--}>120 \mu\text{g m}^{-3}$ ) and much lower background values ( $\sim 5 \mu\text{g m}^{-3}$ ) (Figure S11). Here, we define this segment of the flight as ‘near-field’ (NF) (figure 4(e)). While there was a large step-change in CO and PM<sub>2.5</sub> measurements, there were no clear changes in the measured O<sub>3</sub> concentrations. Before the NF flight segment, O<sub>3</sub> concentrations ranged between 45–85 ppbv, when the aircraft was north-northeast-east of Saddleworth Moor (i.e.  $\sim 10:30\text{--}11:00$  UTC, figures 4(a), (d) and (e)). The NF O<sub>3</sub> concentrations are slightly lower, ranging between 45–80 ppbv.

In the ‘downwind’ (DW) flight segment (approximately 12:00–13:00 UTC—figure 4(e)), the aircraft made plume measurements over the Irish Sea. Here, the aircraft flew between 250–1000 m making multiple passes in and out of the plume. This can be clearly seen in Figures 4(c) and (d) where there are sudden step-changes in CO (100–115 ppbv to > 150 ppbv) and O<sub>3</sub> (50–60 to > 80 ppbv) concentrations with change in altitude. Figures 4(e), S10 and S11 indicate this even more clearly, with CO, O<sub>3</sub>, NO<sub>2</sub> and PM<sub>2.5</sub> concentrations varying between 100–300 ppbv, 45–80 ppbv,  $\sim 1\text{--}8$  ppbv and  $\sim 5\text{--}130 \mu\text{g m}^{-3}$ , respectively, as the aircraft samples the composition in and out of the plume. To isolate in and out of plume concentrations, a CO threshold of 125 ppbv was used to define plume from background concentrations (purple dashed line—Figure 4(e)).

Figure 5 shows CO, O<sub>3</sub> and NO<sub>2</sub> concentrations sub-sampled ‘in-plume’ and ‘out of plume’ (based on the CO 125 ppbv threshold) for the NF and DW flight segments. In the NF, the median CO concentrations are substantially larger ‘in-plume’ than ‘out of plume’ at approximately 725 (220–860, 25th–75th percentiles) ppbv and 107 (104–111) ppbv, respectively. In the DW flight segment, median CO concentrations are substantially lower ‘in-plume’ at approximately 190 (90–260) ppbv, while ‘out of plume’ concentrations are slightly larger (111, 102–115 ppbv) than the NF ‘out of plume’. Again, the same pattern is seen in the results for PM<sub>2.5</sub> (Figure S12). NF ‘in-plume’ concentrations are also much larger for PM<sub>2.5</sub> ( $55.9 \mu\text{g m}^{-3}$ ,  $14.1\text{--}71.8 \mu\text{g m}^{-3}$ ) than the ‘out-of-plume’ median ( $7.5 \mu\text{g m}^{-3}$ ,  $5.8\text{--}10.0 \mu\text{g m}^{-3}$ ). PM<sub>2.5</sub> is also substantially lower DW ‘in-plume’





( $18.43 \mu\text{g m}^{-3}$ ) than NF ‘in-plume’ ( $55.9 \mu\text{g m}^{-3}$ ) and DW ‘in-plume’ ( $18.43, 11.1$  and  $28.2 \mu\text{g m}^{-3}$ ) is also higher than DW ‘out-of-plume’ ( $7.15, 4.47$  and  $9.61 \mu\text{g m}^{-3}$ ).

NF O<sub>3</sub> is larger ‘out-of-plume’ (68, 47–76 ppbv) than ‘in-plume’ (60, 58–61 ppbv). This is consistent with other studies, which show that fire plumes decrease local O<sub>3</sub> concentrations, primarily through titration with freshly emitted NO (Verma *et al*). The opposite occurs for NO<sub>2</sub> where concentrations are larger ‘in-plume’ (2.05, 1.9–2.2 ppbv) than ‘out-of-plume’ (0.9, 0.1–2.1 ppbv). However, the ‘out of plume’ NO<sub>2</sub> range (10th–90th percentiles) is much larger with concentrations peaking above 5 ppbv as the NF NO<sub>2</sub> ‘in-plume’ sample size is small with less spread ( $n = 27$ ). In the DW, O<sub>3</sub> concentrations show enhancements ‘in-plume’ when compared with the NF. DW ‘in-plume’ concentrations are 66 (61–70) ppbv, this is substantially larger than the DW ‘out of plume’ concentrations (O<sub>3</sub> is 59 (57–63) ppbv). This enhancement compared with the surrounding air mass is suggestive of production of O<sub>3</sub> ‘in-plume’ with distance away from the Saddleworth Moor. However, this O<sub>3</sub> enhancement may also be influenced by downwind NO<sub>x</sub> sources (i.e. Liverpool and Manchester). The DW NO<sub>2</sub> concentrations are larger ‘in-plume’ (3.2 (2.1–4.1) ppbv) than ‘out of plume’ (1.2 (0.8–1.8) ppbv), while also

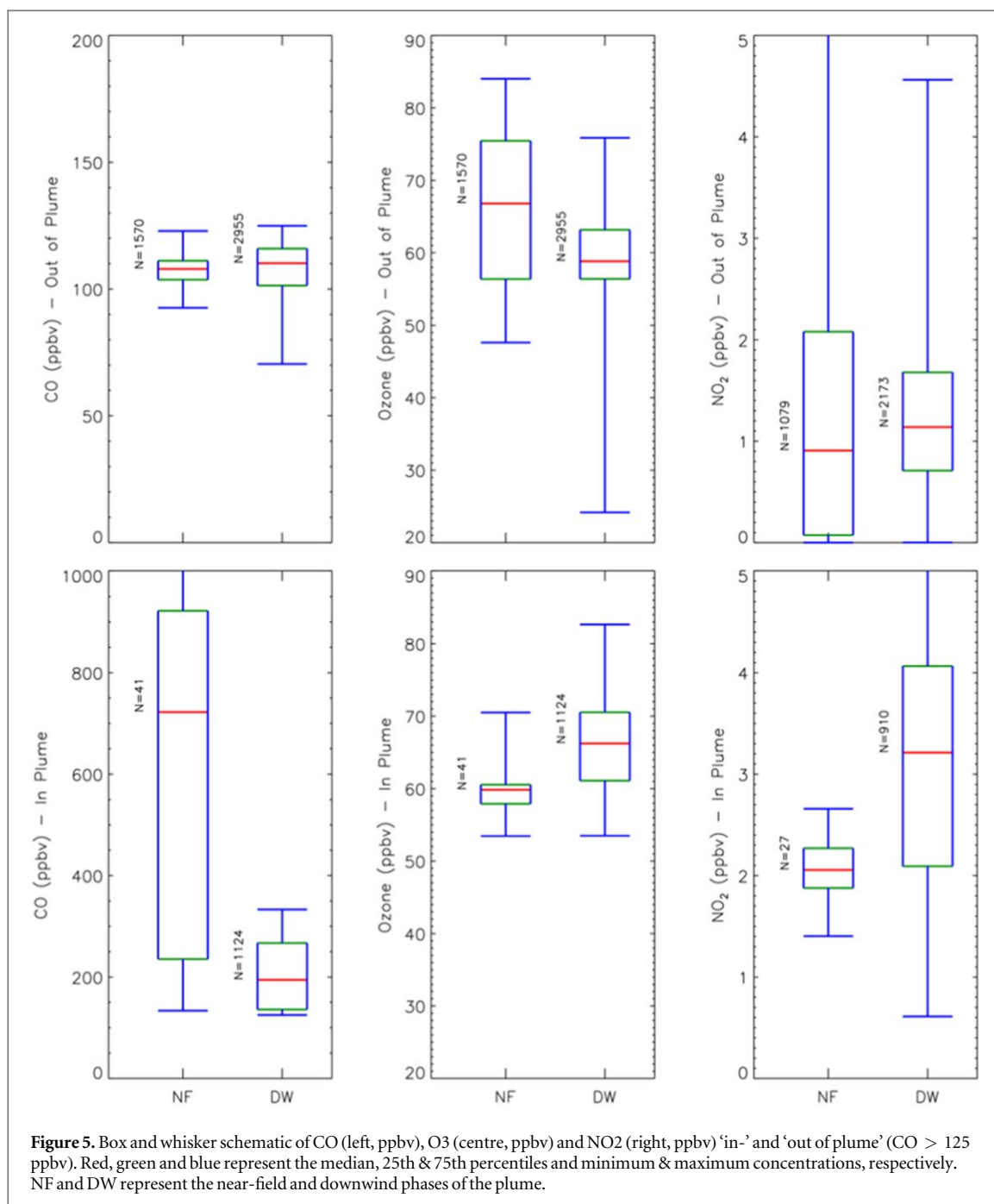
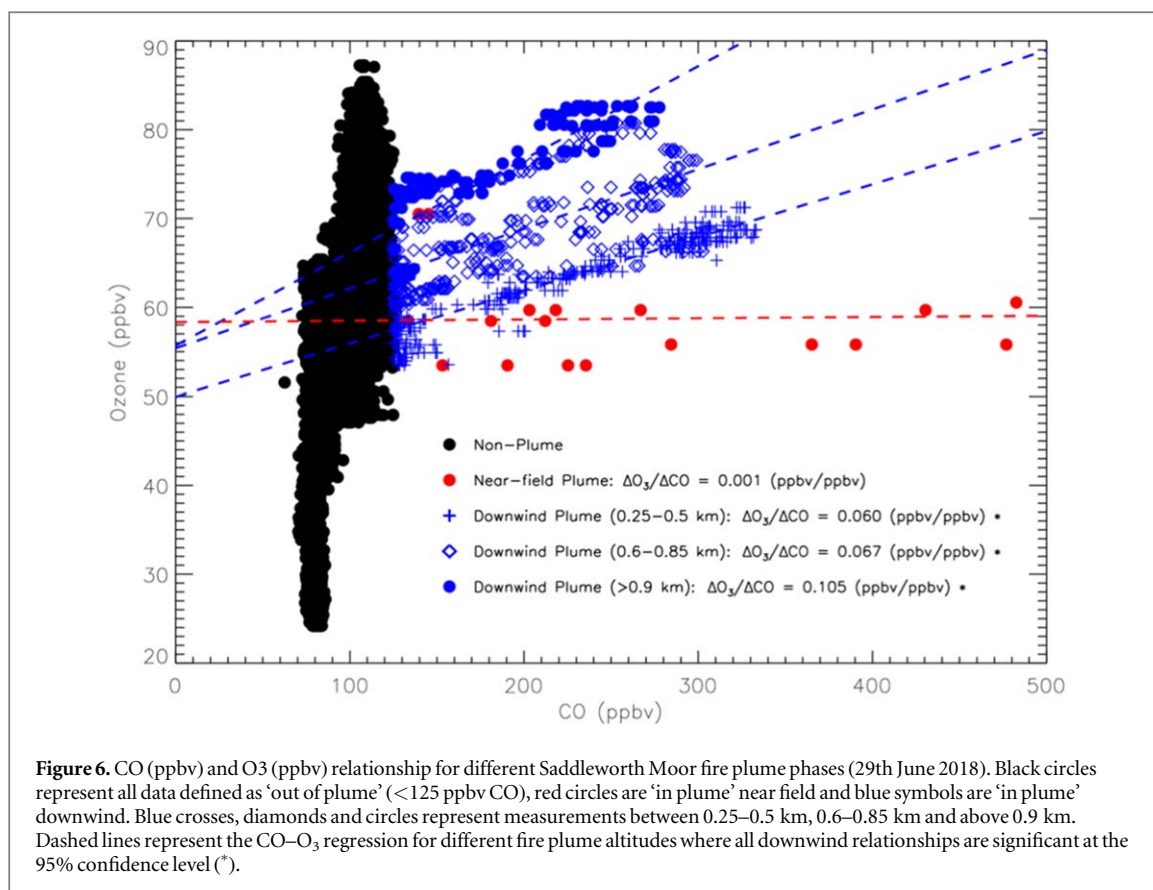


**Figure 5.** Box and whisker schematic of CO (left, ppbv), O<sub>3</sub> (centre, ppbv) and NO<sub>2</sub> (right, ppbv) 'in-' and 'out of plume' (CO > 125 ppbv). Red, green and blue represent the median, 25th & 75th percentiles and minimum & maximum concentrations, respectively. NF and DW represent the near-field and downwind phases of the plume.

larger than the NF 'in-plume' concentrations of 2.05 (1.9–2.2) ppbv. This enhancement of NO<sub>2</sub> concentrations 'in-plume' corroborates the satellite TCNO<sub>2</sub> results in Figure 3, but also the larger DW NO<sub>2</sub> levels. To determine if these pollutant samples were significantly different from each other, the student t-test was used to compare the mean NF 'in-plume' with NF 'out of plume', NF 'in-plume' with DW 'in-plume' and DW 'in-plume' with DW 'out of plume' for each pollutant separately. Overall, we found that all combinations were significantly different for each pollutant at the 95% CL. Thus, concentrations of NO<sub>2</sub>, O<sub>3</sub>, PM<sub>2.5</sub> and CO within the plume are statistically significantly enhanced compared to outside of the plume in NF and DW locations. Alongside this, concentrations are statistically significantly enhanced within the plume NF compared to within the plume DW.

### 3.4.2. 'In Plume' ozone production near-field and downwind

To quantify the enhancement of 'in-plume' O<sub>3</sub> with distance from source, we have used a similar approach to Arnold *et al* (2015) and Jaffe and Wigder (2012). The linear fit between CO and O<sub>3</sub> concentrations was determined for the NF (red symbols) and DW (blue symbols) flight segments (Figure 6), where measurements with CO concentrations < 125 ppbv were excluded (black circles). NF CO ranges between 125 to > 500 ppbv (i.e. CO data > 500 ppbv is used for the statistics, but not plotted to clearly display the DW relationship), whereas



O<sub>3</sub> remains between 53–60 ppbv (note two points peak at ~70 ppbv). The O<sub>3</sub> enhancement, as a function of CO concentration, for the NF is  $\Delta O_3 / \Delta CO = 0.001$  ppbv/ppbv indicating no clear O<sub>3</sub> enhancement with increasing CO. In the DW flight segment there are three distinct positive CO:O<sub>3</sub> slopes at approximately 0.25–0.5 km (crosses), 0.6–0.85 km (diamonds) and above 0.9 km (circles) altitudes. Here, the O<sub>3</sub> enhancements are  $\Delta O_3 / \Delta CO = 0.060$ , 0.067 and 0.105 ppbv/ppbv, respectively, all of which are significant at the 95% CL (i.e. the trends lie outside of the variation observed in the data (outside of  $\pm 2$  standard deviations)). This indicates a significant enhancement of ‘in-plume’ O<sub>3</sub> production increasing with altitude. One likely reason for the larger  $\Delta O_3 / \Delta CO$  rate with altitude is that there is more photochemical production of ozone at top of the plume (i.e. incoming solar radiation reaches this part of the plume first and is attenuated further into the plume) (Jaffe and Wigder, 2012). However, we do not have the detailed chemical measurements necessary to test this hypothesis. Though NO<sub>2</sub> is enhanced DW from urban sources, the  $\Delta O_3 / \Delta CO$  variation with altitude is predominantly from the Saddleworth Moor fires. As shown in Figures 4 and S10, there is a strong correlation with enhancements in all pollutants as the aircraft flies in and out of the plume (also see SM7). The  $\Delta NO_2 / \Delta CO$  ratio (not shown here) has the opposite pattern to  $\Delta O_3 / \Delta CO$  ratio and decreases with height. This potentially suggests that the anthropogenic signal is reducing with altitude or that NO<sub>2</sub> is being processed more quickly with more active photochemistry. However, to accurately diagnose the influence of anthropogenic and fire NO<sub>x</sub> sources on O<sub>3</sub> production, a high-resolution regional modelling frame work is required, which is beyond the scope of this study.

### 3.4.3. Back trajectories

Backward trajectories from the NOAA HYbrid Single-Particle Lagrangian Integrated Trajectory model (HYSPLIT) (Stein *et al* 2015) released from the aircraft sampling regions near-field and downwind can assist estimating the age of air mass which the smoke plume was in when pollutants were sampled. Trajectories were released from the most northerly and southerly points of the near-field (2.2 °W, 53.75 °N at 1100 UTC and 1.9 °W, 53.25 °N at 1200 UTC) and downwind (3.4 °W, 53.75 °N at 1200 UTC and 3.4 °W, 52.75 °N at 1300 UTC) sections of the flight from a range of altitudes during these profiles (500, 750 & 1000 m and 250, 500 and 1000 m, respectively) (Figure S6). The results of the back-trajectory analysis indicate the air mass which near-field samples were taken from was likely 30 min—1 h in age, showing little variation in age with changes in sample height (500, 750 and 1000 m). The air mass of the downwind samples was likely 2–7 h in age, with the age of the

air mass decreasing with increasing altitude (250, 500 and 1000 m) in the northernmost (southernmost) sample location from 4–6, 3–4 and 2–3 h (6–7, 4–5 and 3–4 h).

#### 3.4.4. Deriving CO emissions from the fires

To determine CO emissions from the Saddleworth Moor fires, we consider the cross section made by the aircraft through the plume on June 29th (see figure S13). Here, the plume has an approximate width and thickness of 4482 m and 52 m, respectively. The fire emissions were calculated by:

$$E_{CO} = \overline{\Delta CO} \bar{w} h d \quad (1)$$

where  $E_{CO}$  ( $\text{kg s}^{-1}$ ) represents the emissions of CO,  $\overline{\Delta CO}$  ( $\text{kg m}^{-3}$ ) is the mean fire enhancement between the ‘in-plume’ and ‘out of plume’ CO concentrations,  $\bar{w}$  ( $\text{m s}^{-1}$ ) is the mean wind speed at the flight altitude (assumed to be in the direction of plume flow and perpendicular to the aircraft flight path),  $h$  (m) is the plume thickness and  $d$  (m) is the plume width. The limitations of this approach are the assumptions that  $\bar{w}$  is representative of the full plume wind speed, that the plume cross-section is regular, and the estimate values of  $h$  and  $d$  (the aircraft might not have included the entire plume in the transect). Here,  $\bar{w} = 7.31 \text{ m s}^{-1}$  and  $\overline{\Delta CO} = 6.4 \times 10^{-7} \text{ kg m}^{-3}$ , so  $E_{CO} = 1.07 \text{ kg s}^{-1}$ . To estimate the uncertain range of this emission rate, we perturb the values of  $h$  and  $d$  by 50% (these variables represent the largest source of uncertainty) and use lower and upper limits of  $\bar{w}$  and  $\overline{\Delta CO} \pm 1.0$  standard deviation. This provides a range of  $E_{CO} = 1.07 (0.07\text{--}4.69) \text{ kg s}^{-1}$ , which is in reasonable agreement with remote sensing estimates from the Global Fire Assimilation System (GFAS,  $0.54 \text{ kg s}^{-1}$ ) and Fire INventory from NCAR (FINN,  $2.15 \text{ kg s}^{-1}$ ). When this is repeated for  $\text{CO}_2$ , also measured during the aircraft campaign,  $E_{\text{CO}_2} = 13.7 (1.73\text{--}50.1) \text{ kg s}^{-1}$  while GFAS and FINN have emission rates of  $7.84 \text{ kg s}^{-1}$  and  $33.1 \text{ kg s}^{-1}$ , respectively.

## 4. Discussion and conclusions

Historically, the UK is prone to relatively small vegetation fires (e.g. in comparison to tropical and other boreal fires, Van Der Werf *et al* (2017)), often used in moorland burning for the purposes of agricultural grazing (Yallop *et al* 2006, Davies *et al* 2016). However, in recent years, the UK has experienced several substantially larger fires which have gained much media interest and resulted in the evacuation of surrounding populated areas. In this study, we have successfully used ground-based observations, state-of-the-art satellite and aircraft measurements to quantify the impact of the Saddleworth Moor and Winter Hill fires on regional atmospheric composition and air quality.

Using ground based observations, the impact of pollutants from the fire can be quantified at the surface. Pollutants from the fire were transported westwards during the peak of the fires (27th, 29th and 30th June) over large populations (e.g. Manchester). Consequently, the fire had a significant impact on  $\text{PM}_{2.5}$  concentrations in Manchester and in regions further afield (including Wigan—50 km away). Surface  $\text{PM}_{2.5}$  during the fires was 4–5.5 higher than average and dominated by the non-volatile  $\text{PM}_{2.5}$  fraction. Since concentrations were up to 2 times the WHO recommended guideline limit ( $25 \mu\text{g m}^{-3}$ ) there are likely to have been considerable negative health impacts for individuals exposed, particularly for those with underlying health conditions.

The unprecedented spatial resolution of the new S5P TROPOMI satellite instrument now allows us to detect trace gases from such fires. The time-evolution of total column carbon monoxide (TCCO) measurements during June 25th–30th shows the westward propagation of the Saddleworth Moor fire plume out towards the Irish Sea over the highly populated cities of Manchester and Liverpool. By using quantitative classification of the fire plume (i.e. TCCO concentration and fire radiative power, FRP), we have isolated a significant enhancement in tropospheric column  $\text{NO}_2$  ( $\text{TCNO}_2$ ), a key air pollutant, on top of the enhanced anthropogenic signal from prevailing anticyclonic meteorological conditions (i.e. accumulation of pollutants over source regions). Measurements from the FAAM aircraft flight on June 29th support this, with clear enhancement of boundary layer ( $<1$  km) CO concentrations within the plume. Near Saddleworth Moor, in-plume CO and  $\text{PM}_{2.5}$  measurements peak at over 1500 ppbv and  $127.5 \mu\text{g m}^{-3}$ , while downwind of the plume over the Irish Sea they are somewhat lower at 200–400 ppbv and  $96.1 \mu\text{g m}^{-3}$ . The opposite occurs for ozone ( $\text{O}_3$ ) where the downwind plume shows a significant increase, highlighting its downwind production. Based on  $\text{CO}:\text{O}_3$  correlations within the plume, the  $\text{O}_3$  production increases significantly from  $\Delta\text{O}_3/\Delta\text{CO} = 0.001$  ppbv/ppbv near-field to  $\Delta\text{O}_3/\Delta\text{CO} = 0.060\text{--}0.105$  ppbv/ppbv (depending on the altitude between 250–1000 m) downwind. Our estimates lie within the range of values found in previous studies of similar fires (boreal region mean: 0.018–0.15) (Jaffe and Wigder, 2012). Though urban sources of  $\text{NO}_x$  (i.e. Manchester and Liverpool) may also be contributing to the DW  $\text{O}_3$  enhancements as has been found in previous studies of wildfires near highly populated urban areas (McKeen *et al* 2002, Morris *et al* 2006). Emission rates from Saddleworth Moor, during the smouldering stage of the fire’s life cycle, are estimated to be  $1.07 (0.07\text{--}4.69) \text{ kg s}^{-1}$  and  $13.7 (1.73\text{--}50.1) \text{ kg s}^{-1}$  for CO and  $\text{CO}_2$ , respectively. This  $\text{CO}_2$  emission rate is similar to those of the Grangemouth (near

Edinburgh) or Enfield (north of London) power stations ( $\sim 16.0 \text{ kg s}^{-1}$ ; National Atmospheric Emissions Inventory NAEI (2016)).

We have shown that the Saddleworth Moor and Winter Hill fires produced large quantities of some key air pollutants, including  $\text{O}_3$ ,  $\text{PM}_{2.5}$  and  $\text{CO}$ , which were transported over Manchester and Liverpool yielding a substantial degradation in AQ. In the future, with accelerating climate change leading to enhanced temperatures and drought conditions within the UK (Guerreiro *et al* 2018), wildfires are likely to become more frequent and intense (Albertson *et al* 2010) yielding more hazardous AQ situations in nearby populated areas. Therefore, work is required to accurately determine the surface enhancement in air pollutant concentrations from such fires. As the surface monitoring network (Automated Urban and Rural Network, DEFRA 2014) is sparse, satellite observations and modelling can play an important role. Future work is also needed to assess the corresponding health impacts of exposure to air pollutants from wildfires.

## Acknowledgments

This work was supported by the UK Natural Environment Research Council (NERC) by providing funding for the National Centre for Earth Observation (NCEO) through grant number NE/R016518/1. The contribution of Alberto Sanchez-Marroquin has been supported by the European Research Council (MarineIce (grant no. 648661)).

Surface pressure reanalysis charts from the UK Met Office were accessed from University of Leeds archive. Surface  $\text{PM}_{2.5}$  concentration observations were taken from the AURN network via <https://uk-air.defra.gov.uk/>. The TROPOMI total column  $\text{CO}$  and tropospheric column  $\text{NO}_2$  data were obtained from ESA's Copernicus Open Access Hub (<https://scihub.copernicus.eu/>) and the Tropospheric Emissions Monitoring Internet Service (TEMIS, <http://temis.nl/airpollution/no2.html>), respectively. MODIS fire radiative power (FRP) data was provided by the ECMWF Global Fire Assimilation System (<https://apps.ecmwf.int/datasets/data/cams-gfas/>). ECMWF ERA-Interim meteorological reanalysis data came from <https://apps.ecmwf.int/datasets/data/interim-full-daily/levtype=sfc/>. The Saddleworth Moor aircraft data were taken using the Facility for Airborne Atmospheric Measurements (FAAM) BAe-146–301 Large Atmospheric Research Aircraft and are available from the Centre for Environmental Data Analysis (CEDA) at <https://old.faam.ac.uk/index.php/data>. The authors also gratefully acknowledge the NOAA Air Resources Laboratory (ARL) for the provision of the HYSPLIT transport and dispersion model and/or READY website (<https://ready.noaa.gov>) used in this publication.

## ORCID iDs

A M Graham  <https://orcid.org/0000-0003-2349-3787>

J B McQuaid  <https://orcid.org/0000-0001-8702-0415>

A Sanchez-Marroquin  <https://orcid.org/0000-0003-4510-4551>

## References

- AEAT 2009 QA/QC Procedures for the UK Automatic Urban and Rural Air Quality Monitoring Network (AURN). Report to Defra and the Devolved Administrations, AEAT/ENV/R2837. Accessed 09/01/2020/ Available from: [https://uk-air.defra.gov.uk/assets/documents/reports/cat13/0910081142\\_AURN\\_QA\\_QC\\_Manual\\_Sep\\_09\\_FINAL.pdf](https://uk-air.defra.gov.uk/assets/documents/reports/cat13/0910081142_AURN_QA_QC_Manual_Sep_09_FINAL.pdf)
- Albertson K, Aylen J, Cavan G and McMorrow J 2010 Climate change and the future occurrence of moorland wildfires in the Peak District of the UK *Climate Research* **45** 105–18
- Arnold S R *et al* 2015 Biomass burning influence on high-latitude tropospheric ozone and reactive nitrogen in summer 2008: a multi-model analysis based on POLMIP simulations *Atmos. Chem. Phys.* **15** 6047–68
- Bain C G *et al* 2011 IUCN UK Commission of Inquiry on Peatlands. [Online]. Edinburgh: IUCN UK Peatland Programme. [Date Accessed: 01–04–2019]. Available from: [http://iucn-uk-peatlandprogramme.org/sites/www.iucn-uk-peatlandprogramme.org/files/IUCN%20UK%20Commission%20of%20Inquiry%20on%20Peatlands%20Full%20Report%20spv%20web\\_1.pdf](http://iucn-uk-peatlandprogramme.org/sites/www.iucn-uk-peatlandprogramme.org/files/IUCN%20UK%20Commission%20of%20Inquiry%20on%20Peatlands%20Full%20Report%20spv%20web_1.pdf)
- BBC 2018 Saddleworth Moor fire is out after more than three weeks. BBC News. [Online]. 18-07-2018. [Date accessed: 10-03-2019]. Available from: <https://bbc.co.uk/news/uk-england-manchester-44880331>
- Boersma K F *et al* 2011 An improved tropospheric  $\text{NO}_2$  column retrieval algorithm for the Ozone Monitoring Instrument *Atmos. Meas. Tech.* **4** 1905–28
- Bravo A H, Sosa E R, Sanchez A P, Jaimes P M and Saavedra R M I 2002 Impact of wildfires on the air quality of Mexico City, 1992–1999 *Environ. Pollut.* **117** 243–53
- Center for International Earth Science Information Network—CIESIN - Columbia University 2018 *Gridded Population of the World, Version 4 (GPWv4): Population Count, Revision 11*. (Palisades, NY: NASA Socioeconomic Data and Applications Center (SEDAC)). <https://doi.org/10.7927/H4JW8BX5>. Accessed 10/01/2020. (<https://doi.org/https://doi.org/10.7927/H4JW8BX5>)
- Cheng L, McDonald K M, Angle R P and Sandhu H S 1998 Forest fire enhanced photochemical air pollution. A case-study *Atmos. Environ.* **32** 673–81

- Chowdhury Z, Zheng M, Schauer J J, Sheesley R J, Salmon L G, Cass G R and Russell A G 2007 Speciation of ambient fine organic carbon particles and source apportionment of PM<sub>2.5</sub> in Indian cities *Journal of Geophysical Research: Atmospheres* **112**
- Davies G M *et al* 2016 The role of fire in UK peatland and moorland management: the need for informed, unbiased debate *Philosophical Transactions of the Royal Society B: Biological Sciences* **371** 20150342
- Day R and Green C 2018 The devastating toll of this summer's moorland wildfires has been revealed - as firefighters tackle another blaze. Manchester Evening News. [Online]. 27–07–2018. [Date accessed: 10–03–2019]. Available from: <https://manchestereveningnews.co.uk/news/greater-manchester-news/winter-hill-saddleworth-moorland-fires-14955626>
- Department for Environment, Food and Rural Affairs (DEFRA) 2008 Report: Site Operational Procedures for TEOM FDMS Analysers. AEAT/ENV/R/2750, DEFRA. Accessed 09/01/2020. Available at: [https://uk-air.defra.gov.uk/assets/documents/reports/cat06/0903121612\\_FDMS\\_LSO\\_manual\\_v2.pdf](https://uk-air.defra.gov.uk/assets/documents/reports/cat06/0903121612_FDMS_LSO_manual_v2.pdf)
- Department for Environment, Food and Rural Affairs (DEFRA) 2019 Automatic Urban and Rural Network. [Online]. [Date Accessed: 10–01–2019]. Available from: <https://uk-air.defra.gov.uk/networks/network-info?view=urn>
- Garane K *et al* 2019 TROPOMI/S5P total ozone column data: global ground-based validation and consistency with other satellite missions *Atmos. Meas. Tech.* **12** 5263–87
- Gerbig C, Schmitgen S, Kley D, Volz-Thomas A, Dewey K and Haaks D 1999 An improved fast-response vacuum-UV resonance fluorescence CO instrument *Journal of Geophysical Research: Atmospheres* **104** 1699–704
- Guerreiro S B, Dawson R J, Kilsby C, Lewis E and Ford A 2018 Future heat-waves, droughts and floods in 571 European cities *Environ. Res. Lett.* **13** 034009
- Hamilton D S, Hantson S, Scott C E, Kaplan J O, Pringle K J, Nieradzki L P, Rap A, Folberth G A, Spracklen D V and Carslaw K S 2018 Reassessment of pre-industrial fire emissions strongly affects anthropogenic aerosol forcing *Nat. Commun.* **9** 3182
- Harris N R *et al* 2017 Coordinated airborne studies in the tropics (CAST) *Bull. Am. Meteorol. Soc.* **98** 145–62
- Helas G and Pienaar J J 1996 The influence of vegetation fires on the chemical composition of the atmosphere *S. Afr. J. Sci.* **92** 132–6
- Hu Y, Fernandez-Anez N, Smith T E and Rein G 2018 Review of emissions from smouldering peat fires and their contribution to regional haze episodes *International Journal of Wildland Fire* **27** 293–312
- Information Officer, Greater Manchester Combined Authority (GMCA) 2019 Response to Freedom of Information Request 1920-057. Unpublished
- Jaffe D A and Wigder N L 2012 Ozone production from wildfires: A critical review *Atmos. Environ.* **51** 1–10
- Konov I B, Beekmann M, Kuznetsova I N, Yurova A and Zvyagintsev A M 2011 Atmospheric impacts of the 2010 Russian wildfires: integrating modelling and measurements of an extreme air pollution episode in the Moscow region *Atmos. Chem. Phys.* **11** 10031
- Lambert J-C *et al* 2019 Quarterly validation report of the copernicus sentinel-5 precursor operational data products—#05: April 2018—November 2019 *S5P MPC Routine Operations Consolidated Validation Report series Issue #05, Version 05.0.1* **151**
- Lee J D, Moller S J, Read K A, Lewis A C, Mendes L and Carpenter L J 2009 Year-round measurements of nitrogen oxides and ozone in the tropical North Atlantic marine boundary layer *Journal of Geophysical Research: Atmospheres* **114**
- Liu Y, Goodrick S and Heilman W 2014 Wildland fire emissions, carbon, and climate: Wildfire–climate interactions *Forest Ecology and Management* **317** 80–96
- Lobert J M and Warnatz J 1993 Emissions from the combustion process in vegetation *Fire in the Environment* **13** 15–37
- McKee S A, Wotawa G, Parrish D D, Holloway J S, Buhr M P, Hübler G, Fehsenfeld F C and Meagher J F 2002 Ozone production from Canadian wildfires during June and July of 1995 *Journal of Geophysical Research: Atmospheres* **107** ACH-7
- Moore D P 2019 The October 2017 red sun phenomenon over the UK *Weather* **74** (10) 348–53
- Morris G A *et al* 2006 Alaskan and Canadian forest fires exacerbate ozone pollution over Houston, Texas, on 19 and 20 July 2004 *Journal of Geophysical Research: Atmospheres* **111** D24S03
- National Atmospheric Emissions Inventory (NAEI) 2016 Maps and Emissions Datasets. [Online]. [Date Accessed: 14–07–2018]. Available from: [http://naei.beis.gov.uk/data/map-uk-das?pollutant\\_id=2&emiss\\_maps\\_submit=naei-20190625105934](http://naei.beis.gov.uk/data/map-uk-das?pollutant_id=2&emiss_maps_submit=naei-20190625105934)
- Núñez X C, Ruiz L V and García C G 2014 Black carbon and organic carbon emissions from wildfires in Mexico *Atmósfera* **27** 165–72
- Peterson D A, Campbell J, Hyer E, Fromm M, Kablick G, Cossuth J and DeLand M 2018 Wildfire-driven thunderstorms cause a volcano-like stratospheric injection of smoke. *Climate and Atmospheric Science* **1** 30
- Phuleria H C, Fine P M, Zhu Y and Sioutas C 2005 Air quality impacts of the October 2003 Southern California wildfires *J. Geophys. Res.: Atmospheres* **110**
- Pidd H and Rawlinson K 2018 Saddleworth Moor fire declared major incident as residents evacuated. The Guardian. [Online]. 27–06–2018. [Date accessed: 07–03–2019]. Available from: <https://theguardian.com/uk-news/2018/jun/27/manchester-moorland-fire-declared-a-major-incident-by-police>
- Pope R J, Arnold S R, Chipperfield M P, Latter B G, Siddans R and Kerridge B J 2018 Widespread changes in UK air quality observed from space *Atmos. Sci. Lett.* **19** 817
- Pope R J, Graham A M, Chipperfield M P and Veefkind J P 2019 High resolution satellite observations give new view of UK air quality *Weather* **74** (9) 316–320
- Pope R J, Savage N H, Chipperfield M P, Arnold S R and Osborn T J 2014 The influence of synoptic weather regimes on UK air quality: analysis of satellite column NO<sub>2</sub> *Atmos. Sci. Lett.* **15** 211–7
- Pope R J, Savage N H, Chipperfield M P, Ordóñez C and Neal L S 2015 The influence of synoptic weather regimes on UK air quality: Regional model studies of tropospheric column NO<sub>2</sub> *Atmos. Chem. Phys.* **15** 11201–15
- Reddington C L, Butt E W, Ridley D A, Artaxo P, Morgan W T, Coe H and Spracklen D V 2015 Air quality and human health improvements from reductions in deforestation-related fire in Brazil *Nat. Geosci.* **8** 768
- Reddington C L, Yoshioka M, Balasubramanian R, Ridley D, Toh Y Y, Arnold S R and Spracklen D V 2014 Contribution of vegetation and peat fires to particulate air pollution in Southeast Asia *Environ. Res. Lett.* **9** 094006
- Remer L A *et al* 2005 The MODIS aerosol algorithm, products, and validation *J. Atmos. Sci.* **62** 947–73
- Rosenberg P D, Dean A R, Williams P I, Dorsey J R, Minikin A, Pickering M A and Petzold A 2012 Particle sizing calibration with refractive index correction for light scattering optical particle counters and impacts upon PCASP and CDP data collected during the Fennec campaign *Atmos. Meas. Tech.* **5** 1147–63
- Roulston C, Paton-Walsh C, Smith T E L, Guérette É A, Evers S, Yule C M, Rein G and Van der Werf G R 2018 Fine particle emissions from tropical peat fires decrease rapidly with time since ignition *Journal of Geophysical Research: Atmospheres* **123** 5607–17
- Rowlinson M J *et al* 2019 Impact of El Niño Southern Oscillation on the interannual variability of methane and tropospheric ozone *Atmos. Chem. Phys. Discuss.* **19** 8669–8686
- Ryder C L *et al* 2015 Advances in understanding mineral dust and boundary layer processes over the Sahara from Fennec aircraft observations *Atmos. Chem. Phys.* **15** 8479–520

- Sommers W T, Loehman R A and Hardy C C 2014 Wildland fire emissions, carbon, and climate: science overview and knowledge needs *Forest Ecology and Management* **317** 1–8
- Stein A F, Draxler R R, Rolph G D, Stunder B J, Cohen M D and Ngan F 2015 NOAA's HYSPLIT atmospheric transport and dispersion modeling system *Bull. Am. Meteorol. Soc.* **96** 2059–77
- Tian D, Hu Y, Wang Y, Boylan J W, Zheng M and Russell A G 2009 Assessment of biomass burning emissions and their impacts on urban and regional PM<sub>2.5</sub>: A Georgia case study *Environmental Science & Technology* **43** 299–305
- Turetsky M R, Benscoter B, Page S, Rein G, Van Der Werf G R and Watts A 2015 Global vulnerability of peatlands to fire and carbon loss *Nat. Geosci.* **8** 11
- Veeffkind J P *et al* 2012 TROPOMI on the ESA Sentinel-5 Precursor: A GMES mission for global observations of the atmospheric composition for climate, air quality and ozone layer applications *Remote Sens. Environ.* **120** 70–83
- Verma S *et al* 2009 Ozone production in boreal fire smoke plumes using observations from the tropospheric emission spectrometer and the ozone monitoring instrument *Journal of Geophysical Research: Atmospheres* **114**
- Van Der Werf G R *et al* 2017 *Global fire emissions estimates during* Earth Syst. Sci. Data **9** 697–720
- Wooster M *et al* 2018 New tropical peatland gas and particulate emissions factors indicate 2015 Indonesian fires released far more particulate matter (but less methane) than current inventories imply *Remote Sensing* **10** 495
- Xu J, Morris P J, Liu J and Holden J 2018 PEATMAP: Refining estimates of global peatland distribution based on a meta-analysis *Catena* **160** 134–40
- Yallop A R, Thacker J I, Thomas G, Stephens M, Clutterbuck B, Brewer T and Sannier C A D 2006 The extent and intensity of management burning in the English uplands *J. Appl. Ecol.* **43** 1138–48